

Research Article

FGF9 is a downstream target of SRY and sufficient to determine male sex fate in ex vivo XX gonad culture

Yi-Han Li¹, Tsung-Ming Chen², Bu-Miin Huang^{1,3}, Shang-Hsun Yang^{1,4}, Chia-Ching Wu^{1,3}, Yung-Ming Lin⁵, Jih-Ing Chuang^{1,4}, Shaw-Jenq Tsai^{1,4} and H. Sunny Sun^{1,6,*}

¹Institute of Basic Medical Sciences, College of Medicine, National Cheng Kung University, Tainan, Taiwan, ²Department and Graduate Institute of Aquaculture, National Kaohsiung University of Science and Technology, Kaohsiung, Taiwan, ³Department of Cell Biology and Anatomy, College of Medicine, National Cheng Kung University, Tainan, Taiwan, ⁴Department of Physiology, College of Medicine, National Cheng Kung University, Tainan, Taiwan, ⁵Department of Urology, National Cheng Kung University Hospital, College of Medicine, National Cheng Kung University, Tainan, Taiwan and ⁶Institute of Molecular Medicine, National Cheng Kung University, Tainan, Taiwan

*Correspondence: Institute of Molecular Medicine, College of Medicine, National Cheng Kung University, 1 University Road, Tainan 70101, Taiwan. Tel: 886-6-235-3535 ext. 3648; Fax: 886-6-209-5845; E-mail: hssun@mail.ncku.edu.tw

Grant Support: This work was supported by the grant from the Ministry of Science and Technology, Taiwan (MOST104-2320-B-006-042 to HSS).

Received 22 January 2020; Revised 2 July 2020; Editorial Decision 27 August 2020; Accepted 3 September 2020

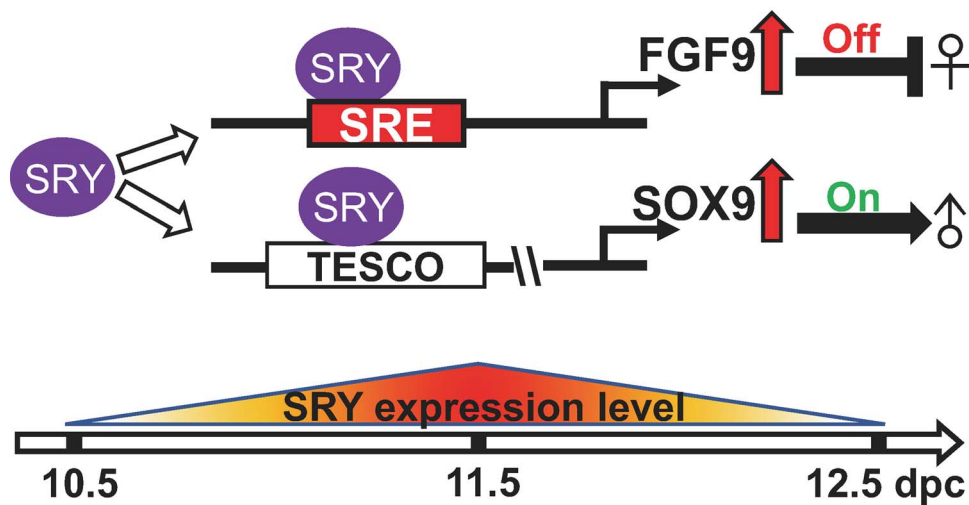
Abstract

Fibroblast growth factor 9 (FGF9) is an autocrine/paracrine growth factor that plays critical roles in embryonic and organ developments and is involved in diverse physiological events. Loss of function of FGF9 exhibits male-to-female sex reversal in the transgenic mouse model and gain of *FGF9* copy number was found in human 46, XX sex reversal patient with disorders of sex development. These results suggested that FGF9 plays a vital role in male sex development. Nevertheless, how *FGF9/Fgf9* expression is regulated during testis determination remains unclear. In this study, we demonstrated that human and mouse SRY bind to –833 to –821 of human *FGF9* and –1010 to –998 of mouse *Fgf9*, respectively, and control *FGF9/Fgf9* mRNA expression. Interestingly, we showed that mouse SRY cooperates with SF1 to regulate *Fgf9* expression, whereas human SRY-mediated *FGF9* expression is SF1 independent. Furthermore, using an ex vivo gonadal culture system, we showed that FGF9 expression is sufficient to switch cell fate from female to male sex development in 12–16 tail somite XX mouse gonads. Taken together, our findings provide evidence to support the SRY-dependent, fate-determining role of FGF9 in male sex development.

Summary Sentence

FGF9 shows a fate-determining role within 6-h time windows during male sex development and SRY directly regulates *FGF9/Fgf9* mRNA expression through binding to the SRY-responsive elements in the *FGF9/Fgf9* promoter region.

Graphical Abstract

Male Sex Determination

Key words: human reproduction, male sexual function, sex determination, sex differentiation, testis, gene regulation, transcriptional regulation, growth factors.

Introduction

The development of two sexes is observed in most animals and is essential for their survival and evolution. However, disorders of sex development are among the most common genetic diseases in humans and are often associated with genital ambiguity [1]. It has been estimated that one in every 100 000 newborn females has a 46 XY male-to-female sex reversal phenotype [2]. For a long while, the SRY gene was thought to be the key factor for testis development [3]; however, only 10–20% of sex reversal patients can be explained by SRY gene mutations [4]. In spite of homologs been found in eutherians, marsupials, and monotremes [5, 6], the SRY gene is only found in mammals. Thus, a handful genes, including SRY-related homeobox protein 9 (SOX9) [7], Wilm tumor 1 (WT1) [8], steroidogenic factor 1 (SF1) [9], nuclear receptor subfamily 0 group B member 1 (NR0B1) [10], and doublesex and mab-3 related transcription factor 1 (DMRT1) [11], have been identified to be involved in the sex determination/differentiation through analyses of human subjects with impaired sex differentiation or knockout mice. However, mutations from these genes account for ~50% of the patients with primary sex determination deficit [12]. These results suggest that genes other than SRY may also play important roles in sex development in the evolution history. In fact, increasing evidences indicate that other players downstream from SRY are sufficient for sex determination, and an imbalanced expression among these genes may cause sex reversal at various magnitudes [13, 14]. Fibroblast growth factor 9 (FGF9) is an autocrine/paracrine growth factor that plays an essential role in embryonic development and physiological controls [15–18]. Knockout of *Fgf9* in the mice resulted in male-to-female sex reversal provides the first evidence to show the involvement of FGF9 in male sex determination [19]. In mouse studies, FGF9 and SOX9 form a positive feedforward loop

to enhance the differentiation of testis [20], whereas a recent study reported a novel mouse *Fgfr2* mutant, the main gonad receptor of FGF9 during sex determination, exhibits complete XY gonad sex reversal [21]. In humans, our previous study demonstrated a strong association between FGF9 polymorphism and male-to-female sex reversal [22] and found aberrant expression of testicular FGF9 in patients with Sertoli cell-only syndrome [23]. Moreover, another study identified a gain of FGF9 copy numbers in one SRY-negative 46, XX male patient [24]. Furthermore, FGF9 has been shown to act as the diffusible conductor to direct center-to-pole expansion of tubulogenesis in mouse testis differentiation [25]. Taken together, these results strongly support the notion that the secreted molecule FGF9 plays a critical role in testis determination by acting as a diffusible conductor for the poleward expansion of tubulogenic programs and testis cord formation in the developing XY gonad. In addition, FGF9 has been shown to rescue the blockage of Sertoli cell differentiation in *ex vivo* XY *Wt1(+KTS)*-null mouse gonad cultures [26]. On the other hand, in cultured XX gonads, it has been shown that exogenous FGF9 alone [20], or in combination with activin and TGF-beta [27], is able to trigger male testis development. Thus, whether expression of FGF9 is sufficient to trigger male sex development in an XX genetic background and results in female-to-male sex reversal is of interest to be illustrated.

As FGF9 signaling induces FGFR2 to relocate into the nucleus and coincides with the expression of nuclear SRY and SOX9 [28], it appears that FGF9 may act downstream of SRY and/or SOX9 to promote embryonic testicular cord formation during testis morphogenesis [17]. Through the use of gain- and loss-of-function experiments, Kim et al. [20] demonstrated that SRY initiates a feedforward loop between SOX9 and FGF9, which upregulates FGF9 and represses WNT4 to establish the testis pathway in the mouse XY gonad. Furthermore, Li et al. [29] applied whole-genome promoter

tiling microarray (chromatin immunoprecipitation [ChIP]-on-Chip) in E11.5 and E12.5 mouse gonad cells revealed that SRY binds to its target genes, including *Fgf9*, to activate testicular differentiation. Nevertheless, the direct proof of SRY-regulated *Fgf9* expression in controlling male sex development remains undetermined. This study set out to define the binding site(s) of SRY on *FGF9* promoter and examine whether FGF9 expression is sufficient to govern male sex fate and to activate male gonad development. Using *ex vivo* 3D culture, we provide evidence to show that FGF9 alone is able to induce testis cord formation in XX gonads within a critical time window of ~6 h (12–16 tail somite). In addition, we identify critical control regions of SRY binding to *FGF9* promoter and establish the regulation of SRY-mediated FGF9 expression in both humans and mice in cellular models. Overall, our data support the notion that SRY binds to *FGF9* promoter to regulate its expression, which is essential to determine male sex fate in early embryonic development.

Materials and methods

Mice and cell lines

Mice used in all experiments were FVB mice obtained from the Laboratory Animal Center at the National Cheng Kung University. Four male and 15 female FVB mice were used in this study. All animal studies were approved by the Animal Welfare Committee of the National Cheng Kung University (IACUC Approval Number: 103096).

Human embryonic kidney 293 (HEK293), embryonic carcinoma (NT2/D1), and African green monkey kidney fibroblast-like (COS7) cells were incubated at 37 °C in a cell incubator containing 5% CO₂ with appropriate culture medium according to the ATCC guidelines.

Primary gonads *ex vivo* 3D culture

The presence of a vaginal plug in the morning was used to indicate mating and was recorded as E0.5. For more precise staging of embryos younger than E12.5, the number of tail somite (ts) posterior to the hind limb bud was used, according to the description in the literature [30]. A total of 52 mouse embryos were collected at 12–18 ts stages for *ex vivo* 3D culture assay. The gonad/mesonephros tissues from 12, 16, and 18 ts stage embryos, approximately equal to E11, E11.25, and E11.5, were collected and placed onto 30 µL Mebiol Gel (MBG-PMW20-1001, Cosmo Bio, Japan) in a 12-well plate. The Mebiol gel was covered by 1 mL Dulbecco minimal essential medium containing 10% heat-inactivated defined fetal bovine serum (FBS) with or without 50 ng/mL recombinant human FGF9 (R&D Systems, USA), and incubated at 37 °C in a cell incubator containing 5% CO₂. Tissues were cultured for 5 days, with daily changes of organ culture media. All organ cultures were replicated at least three times, and more than three individual gonads were collected per age group. After being cultured for 5 days, the gonad/mesonephros tissues were carefully removed from the Mebiol gel and fixed in 4% paraformaldehyde overnight, rinsed twice in 1 mL phosphate-buffered saline (PBS), and then dehydrated in 200 µL 30% sucrose buffer for further analysis. The gonads were photographed under a bright field and were analyzed following immunofluorescence (IF) staining with different cell marker antibodies.

To determine the gender of each individual embryo, the remaining tissues from a given embryo were used for DNA isolation using QIAGEN reagents (QIAGEN, Germany). DNA then underwent Sry polymerase chain reaction (PCR) to a total of 30 cycles (94 °C for 30 s, 54 °C for 30 s, and 72 °C for 30 s per cycle). An amplicon size of

301 bp in 1.8% agarose gel indicated the presence of Y chromosome (Supplementary Table S2).

IF assay and western blot analysis

For the IF assay, the gonads were prepared in cryosections at a thickness of ~7 µm. The primary antibodies of Sox9 (1:2000; AB5535 Chemicon), Amh (1:500; sc-6886 Santa Cruz Biotechnology), Laminin (1:1000; ab11575 Abcam), and Foxl2 (1:500; NB100-1277 Novus Biologicals) were diluted in fresh blocking buffer and incubated with slides at 4 °C overnight. After washing three times with PBS for 5 min at room temperature (RT), slides were incubated for 1 hour (h) with Alexa fluor 488-, 555-conjugated goat anti-rabbit or 555-conjugated rabbit anti-goat (1:1000; Molecular Probes, USA), and DAPI (1:2500; Molecular Probes, USA). A final wash with PBS was performed three times for 5 min at RT. The presence of testicular cord formation was estimated using laminin-, Sox9-, and Amh-stained sections as follows: negative (–), no cord-like structure; slender (±), slight cord-like structure; positive (+), well-defined testicular cords in the gonadal area [31].

For western blot analysis, cells were lysed in RIPA buffer with protease inhibitor (Roche, USA) and protein concentration was estimated by Micro BCA assay (Thermo Fisher Scientific, USA). In total, 30 µg of total cell lysates were run on 10% sodium dodecyl sulfate polyacrylamide gel electrophoresis and blotted onto PVDF membranes. Antibodies against human SRY (1:1000; sc-33168 Santa Cruz Biotechnology) was used and the signals were detected using enhanced chemiluminescence (ECL; Amersham).

Transcription factor binding site prediction

DNA sequences upstream from the transcription start site (TSS) of human *FGF9* (NM_002010.1, ~1949 bp) and mouse *Fgf9* (NM_013518.4, ~1873 bp) were used to predict the presence of putative binding sites for transcription factors (TFs) using online computational tools including TESS (<https://www.cbil.upenn.edu/tess>, Ver1.1) and TFsearch (<http://molsun1.cbrc.aist.go.jp/research/db/TFSEARCH.html>, Ver1.3). The maximum matrix dissimilarity rate was set to 30 and 15 for TESS and TFsearch, respectively, for the prediction of SRY- and SF1-binding sites.

To identify binding sites for influential regulators, we search collections in the ChIP-Atlas database (<https://chip-atlas.org/>), an integrative and comprehensive database for visualizing public ChIP-seq data from over 131000 experiments that have been submitted to the Sequence Read Archives in NCBI, DDBJ, or ENA [32]. To perform the search, antigen class was set to “TFs and others”, cell type class was set to “Gonad” and “Embryonic” (gonad and embryonic associate cell types), and threshold for statistical significance values calculated by peak-caller MACS2 ($-10 \times \log_{10}[\text{MACS2 } Q\text{-value}]$) of 20, 200, 500 were applied.

Plasmid constructs

To clone the promoter regions for further analysis, primers were designed based on the human *FGF9* (NM_002010.1, ~1949 bp) [22] and mouse *Fgf9* (NM_013518.4, ~1873 bp) sequences. Using either sequence-containing or primer-anchored restriction enzyme cutting sites, fragments containing various human SRY-response element (hSRE) and mouse SRY-response element (mSRE) were cloned into the pGL3-basic vector (Promega, USA) for further applications (Supplementary Table S2). For the mutagenesis assay, a mega primer PCR method was used to generate the hSRE-6-binding site mutant

(FGF9 promoter –833/–821 region, [Supplementary Table S2](#)) and clone into the pGL3-basic reporter construct.

To overexpress SRY in the cells, the coding region of human SRY (NM_003140.1, 149–763 bp) was amplified by specific primers ([Supplementary Table S2](#)) and cloned into HindIII and XbaI sites of pcDNA3.1/Myc_His(+)/A vector (Invitrogen, USA). In addition, cDNA clones overexpressing recombinant human SF1 (RC207577), mouse SRY (RC207577), mouse SOX9 (MR227031), and mouse SF1 (RC207577) were purchased from OriGene (OriGene Technologies Inc., Rockville, MD).

Transient transfection and luciferase reporter assay

In total, 500 ng or 1 µg of DNA from the indicated construct plasmid were transfected with lipofectamine 2000 or LTX (Invitrogen, USA) to HEK293 (24-well culture plate, 2×10^5 cells/well) and COS7 (12-well culture plate, 5×10^4 cells/well) in each well. Cells were incubated for 24 h (HEK293) or 48 h (COS7), followed by harvesting with culture cell lysis buffer (Promega, USA) and subjected to luciferase assay (Promega, USA) using Luminometer 20/20 (Turner Biosystems). In parallel, beta-galactosidase activity was assayed using a beta-galactosidase enzyme assay system (Promega, USA) and used to normalize luciferase activity.

Total RNA extraction, reverse-transcription and quantitative real-time PCR

Total RNA was isolated by TRIzol reagent (Invitrogen, USA) and ~2 µg of RNA was reverse transcribed to cDNA by high-capacity cDNA reverse transcription kits (Applied Biosystems) with 50 units of a RNase inhibitor (Promega, USA) in a 50-µL reaction for cDNA synthesis.

Quantitative real-time PCRs of FGF9 (HS00181829-m1), beta-actin (Hs01060665_g1), Luc ([Supplementary Table S2](#)), and 18 s rRNA (4319413E) were carried out by TaqMan assays in a sequence detector (Applied Biosystems). The relative levels of FGF9 and Luc mRNA expression were calculated using the $2^{-\Delta\Delta C_t}$ method and normalized to the expression levels of *beta-actin* and 18 s rRNA.

FGF9 enzyme-linked immunosorbent assay

Culture medium was collected from SRY-overexpressing NT2/D1 cells and analyzed using the FGF9 enzyme-linked immunosorbent assay (ELISA) kit (R&D Systems, USA). The concentration of total protein in the culture medium as loading control was determined by Micro BCA assay (Thermo Fisher Scientific, USA) as described previously [33].

Chromatin immunoprecipitation assay

ChIP assays were conducted in human NT2/D1 cell line that has been reported to express endogenous testis sex determination and differentiation genes [34]. Approximately, 2×10^6 NT2/D1 cells were used in ChIP assays according to the procedure described previously [35]. Antibodies against human SRY and SF1 were used to pull down endogenous SRY and SF1 proteins. Normal rabbit IgG was used as a negative control in the ChIP reaction. After protein digestion by proteinase K at 50 °C for 2 h, DNA was extracted using phenol/chloroform and precipitated by isopropanol. The purified DNA was subjected for PCR with specific primer pairs ([Supplementary Table S2](#)) to amplify indicated regions from the FGF9 and anti-Mullerian hormone (AMH) genes.

Electrophoretic mobility-shift assay

The electrophoretic mobility-shift assays (EMSA) were carried out using biotin-labeled DNA probes targeting FGF9 hSRE-6- and hSRE-8-binding sites ([Supplementary Table S2](#)) and incubated with NT2/D1 cells nuclear extracts according to the published protocol [36]. For the competition assay, 10-, 30-, or 50-fold of an unlabeled oligo ribonucleotide probe was added to the reaction. The biotin-labeled probes were then added for 30 min at RT. For the supershift assays, the nuclear proteins were incubated with human SRY antibody or IgG control for 1 h at RT. The reaction was further incubated with a DNA probe for additional 30 min at RT. The relative band intensities from the blots were quantified by using spot density function with a gel documentation system (Alpha Innotech).

Statistical analysis

All experimental data were analyzed using GraphPad Prism 7.0 (GraphPad Software, Inc., San Diego, CA) and presented as mean \pm standard error of the mean (SEM). Results were further analyzed using Student *t*-test or one-way analysis of variance; the Tukey post hoc test was used when appropriate. To overcome the small sample size, a Fisher exact test (two tailed) was applied to test the stage-dependent differences in the frequency of XX gonads/testis cord formation. The significance level for all statistical tests was set at 0.05.

Results

Human SRY upregulates FGF9 expression by transcriptional activation

Previously, an *in vivo* ChIP-assay study demonstrated that *Fgf9* is a downstream target of SRY in the E11.5 male mouse gonad [29]. It is therefore of interest to assess the transcriptional control of SRY on FGF9 expression in humans. To test this possibility, we measured endogenous FGF9 mRNA and protein expressions under overexpression of human SRY in the NT2/D1 cells ([Figure 1A](#), upper panel). The results show that SRY overexpression significantly elevated FGF9 mRNA to ~1.4-fold ($P < 0.01$, [Figure 1A](#), bottom left). Consequently, an increase of FGF9 protein production to ~1.1–1.5-fold was also found in cells overexpressing recombinant SRY ($P < 0.05$, [Figure 1A](#), bottom right). Next, we cloned the ~2-kb upstream sequences from the TSS of human FGF9 (–1949/216 bp, NCBI accession number: NM_002010.1) into a luciferase reporter gene vector ([Figure 1B](#), upper panel) and cotransfected with the overexpressing SRY construct. By measuring the luciferase activity, our data demonstrated that FGF9 promoter activity significantly elevated in a recombinant SRY dosage-dependent manner ($P < 0.05$, [Figure 1B](#), bottom panel). These results suggest that the level of human SRY is positively associated with the expression of FGF9, perhaps through SRY transcriptional activity.

To assess the possibility that SRY upregulates FGF9 mRNA expression through transcriptional activation, we predicted the SRY-binding sites in the human FGF9 promoter region and obtained a total of eight putative hSRE ([Supplementary Table S1](#), [Figure 1C](#)). In contrast, the prediction of putative SOX9-binding sites within this region resulted in nothing beyond the cutoff score of 85 ([Supplementary Table S1](#)). The functional hSRE was examined by luciferase reporter assays using serial deletion plasmids containing different hSREs ([Figure 1D](#), left panel) in cellular models. The relative luciferase activity was measured and normalized to the full-length construct including hSREs 1–8 (i.e., –1949/216 from

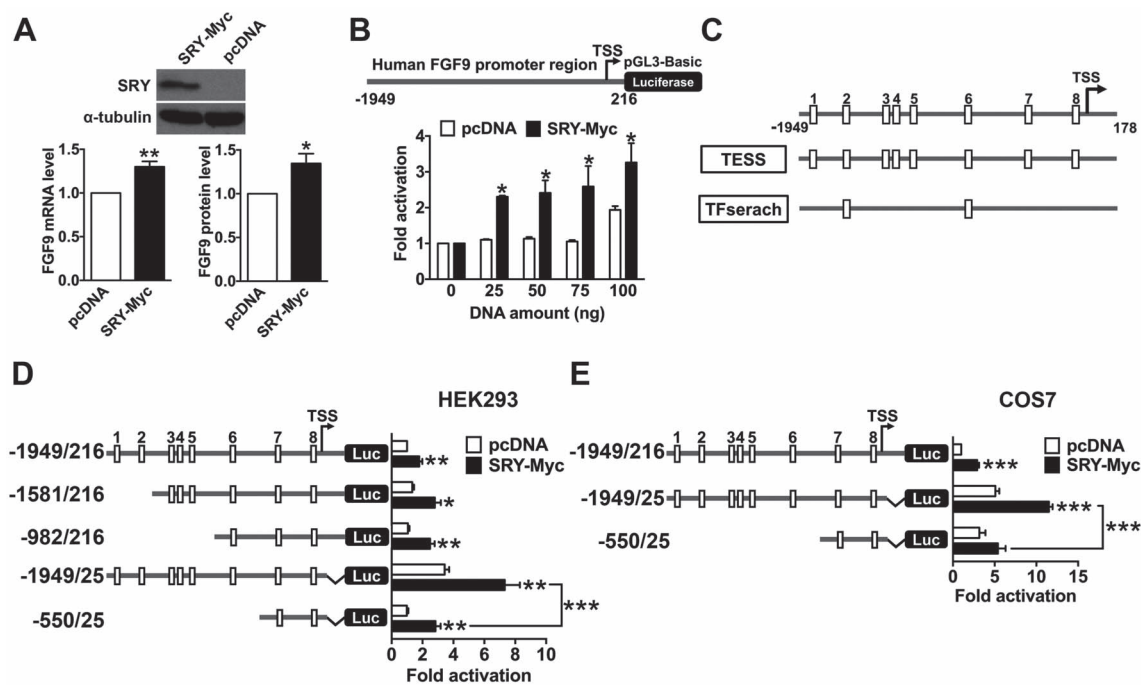


Figure 1. Identification of potential SRY-binding sites in *FGF9* promoter region. (A) Representative western blot showed transient expression of recombinant human SRY–Myc in NT2/D1 cells. Alpha-tubulin was used as a loading control (Upper). Quantitative RT-PCR and ELISA were used to measure *FGF9* mRNA and protein expressions, respectively, in human NT2/D1 cells under overexpression recombinant human SRY. The results showed that ectopic expression of human SRY increased endogenous *FGF9* mRNA (Lower panel, left) and protein (Lower panel, right) in NT2/D1 cells. (B) Luciferase activity assays were performed in cells cotransfected with human *FGF9* reporter plasmid (Upper, –1949/216 from the TSS) and recombinant SRY–Myc or pcDNA construct with different DNA amount (Lower). Luciferase activities were normalized to B-galactosidase activity (see Materials and methods) and compared with no cotransfected plasmids. (C) Diagram of SRY-binding sites (open boxes) predicted using TESS and TFsearch (as indicated) computational tools. The detail information of binding site sequences is provided in [Supplementary Table S1](#). (D and E) Schematic representation of firefly luciferase reporter constructs containing human *FGF9* promoter region with different putative SRY-binding sites (Left). Measurements of luciferase activities in cells cotransfected with reporter constructs and recombinant SRY–MYC were shown in (D) HEK293 and (E) COS7 cells. Luciferase activities were compared with that of full-length construct –1949/216 cotransfected with pcDNA and shown as relative luciferase activity (fold activation, Right). Transcription start site marks the TSS. All experiments have been carried out more than three times and the data were presented as mean \pm SEM, * $P < 0.05$; ** $P < 0.01$; *** $P < 0.001$.

FGF9 TSS) and then cotransfected with pcDNA entry vector in HEK293 cells. Notably, a significant elevation of luciferase activity was observed in all deletion reporter constructs under SRY overexpression, ($P < 0.01$, [Figure 1D](#), right). As the luciferase activities were similar among –1949/216 (hSREs-1-8), –1581/216 (hSREs-3-8), and –982/216 (hSREs-6-8) constructs, the data suggested no functional SRY-binding sites within the indicated regions ([Figure 1D](#)). In agreement with our previous findings [33], removal of the known upstream open reading frame (uORF) from construct –1949/25 drastically raised luciferase activity to ~4-fold and even up to 7.3-fold under SRY expression. Interestingly, a sharp reduction in luciferase activity was obtained for the –550/25 (hSREs-7-8) construct in comparison with the –1949/25 construct under SRY overexpression ($P < 0.001$, [Figure 1D](#)), suggesting that the functional SRY-binding site may be located within this region (hSRE-6). The experiment was replicated in the COS7 cells, where no endogenous SRY can affect the reporter assay results, and the deletion of the putative SRY-binding site resulting in a significant reduction of luciferase activity was confirmed ($P < 0.001$, [Figure 1E](#)). Taken together, these data suggest that the putative hSRE between –833 and –821 from human *FGF9* TSS contributes to the SRY-mediated promoter activity.

SRY binds to *FGF9* promoter and upregulates *FGF9* mRNA expression

Next, we applied a ChIP assay to determine whether endogenous SRY directly interacts with *FGF9* DNA to promote its mRNA expression. Fragmented chromatin was prepared from NT2/D1 cells, a cell line has been reported that express testis sex determination and differentiation genes [34] and pulled down by anti-SRY antibody. This was followed by PCR with specific primer pairs to detect the amount of pulled down chromatin from various putative SRY-binding sites located in the human *FGF9* promoter region ([Figure 2A](#), upper panel). Compared with the IgG control, we found an increase of up to 6-fold in the ChIP–PCR from SRY-pulled down DNA using primer pair targeting hSRE-6 ($P < 0.001$), whereas no differences were detected between SRY- and IgG-ChIP groups using other primer pairs ([Figure 2A](#), bottom panel, [Supplementary Figure S1A](#)). The ChIP–PCR result was in good agreement with the results of the reporter gene, suggesting that human SRY directly interacts with *FGF9* through the hSRE-6 (–833/–821 bp) putative binding site. The protein–DNA interaction was confirmed using EMSA. Using a synthesized oligoprobe containing putative hSRE-6 (–833/–821 bp) sequences, results from the EMSA assay clearly showed that biotin-labeled probes formed three complexes when

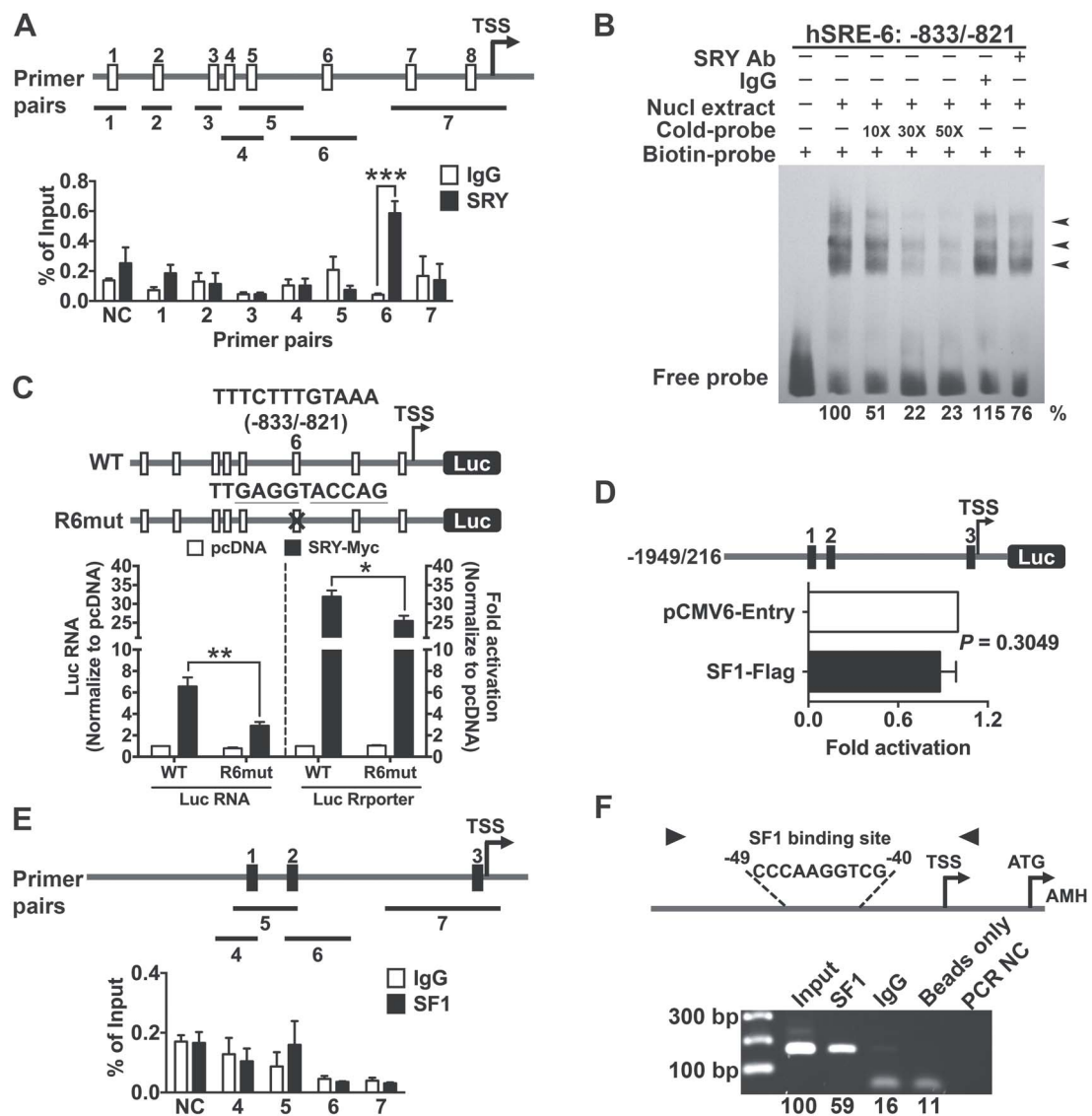


Figure 2. Human SRY, not SF1, directly binds to *FGF9* promoter and upregulates *FGF9* mRNA expression. (A) Schematic representation of ChIP-PCR primer pairs (Upper, black bars) designed to amplify indicated SRY-binding sites (Upper, open boxes). The bar chart presents the quantitative signals in each amplicon normalized to the "Input" and shows SRY relative to the control IgG (Lower). NC was from a primer pair to amplify *FGF9* 3'UTR region and used as a negative control. (B) EMSA was performed with oligonucleotide targeting hSRE-6 833/–821 and SRY antibody. The relative band intensities were quantified by using spot density, normalized to the value of lane 2, and are presented as relative percentage in the bottom of each lane ($n = 3$). From left to right, lanes 1 and 2 probe only and experiment performed with nuclear extract only, respectively. Lanes 3–5 present competition assays with 10-, 30-, or 50-fold of unlabeled probes. Lanes 6–7 show results with additional of IgG or anti-SRY antibody adding to the reaction as negative control and specific DNA–SRY interaction, respectively. Arrowhead indicates protein–DNA interacting bands. (C) hSRE-6 mutagenesis assay. Schematic representation of luciferase reporter constructs (*FGF9* –1949/216) contain wild type (WT, TTTCTTTGTAAA) and hSRE-6 mutant (R6mut, TTGAGGTACCAG) sequences (Upper). Luc RNA expression was measured using quantitative RT-PCR from WT and R6mut constructs cotransfected with pcDNA or SRY–Myc (Lower panel, left). Reporter gene activity is shown as relative luciferase activity (fold activation) normalized to hSRE WT cotransfected with pcDNA (Lower panel, right). (D) Luciferase activities from 1949/216 *FGF9* promoter construct cotransfected with SF1 overexpression plasmid. Schematic representation of the luciferase reporter constructs contains *FGF9* promoter with three predicted SF1-binding sites (Upper). Reporter gene activity is shown as relative luciferase activity (fold activation) normalized to –1949/216 promoter construct cotransfected with pCMV6-Entry (Lower). (E and F) Fragmented chromatin was precipitated by SF1 antibody and PCR with primers targeting (E) *FGF9* and (F) *AMH* promoter region. PCR primer pairs are indicated by black bars (*FGF9*) or arrowhead (*AMH*) (Upper panels). Quantifications of amplicon signals enriched by endogenous SF1 are shown in bar chart (*FGF9*) or percentage to the input (*AMH*) (Lower panels). NC indicates negative control by a primer pair to amplify *FGF9* 3'UTR region. All data are presented as means \pm SEM ($n = 4$). All experiments have been carried out more than three times and the data were presented as mean \pm SEM, * $P < 0.05$; ** $P < 0.01$; *** $P < 0.001$.

incubated with NT2/D1 nuclear extracts (Figure 2B, lanes 1 and 2). The addition of 10X–50X excess of unlabeled probes (cold probe) into biotin-labeled probes competed with the interaction between biotin-labeled probes and nuclear extracts as indicated by the reduction of binding affinity to 51–22% (Figure 2B, lanes 3,

4, and 5). The results indicated that the binding of proteins to the DNA is specific. Furthermore, anti-SRY antibody was used to confirm the binding of SRY to the biotin-labeled oligonucleotides. Compared with the nonspecific IgG control, SRY-specific antibody showed ~25% reduced intensity for the protein–DNA complex

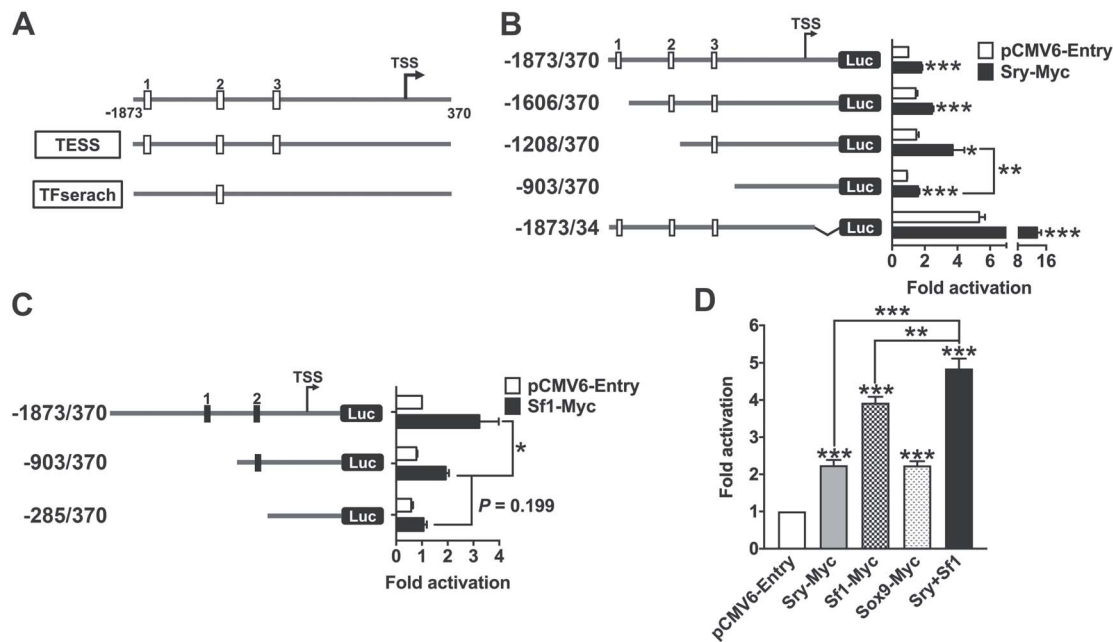


Figure 3. Mouse SRY and SF1 bind to *Fgf9* promoter and cooperatively stimulate its activity. (A) Computational analysis from TESS and TFsearch predicted SRY-binding sites (open boxes) on mouse *Fgf9* promoter region (–1873 to 370 relatives to the TSS). (B) Schematic representation of luciferase reporter constructs contains *Fgf9* promoter with different putative SRY-binding site (mSRE, open boxes, Left). Reporter gene activity is shown as relative luciferase activity (fold activation) normalized to full-length construct (–1873/370, mSRE1-3) cotransfected with pCMV6-Entry (Right). All data are presented as means \pm SEM ($n = 4$), * $P < 0.05$; ** $P < 0.01$; *** $P < 0.001$. (C) Schematic representation of relative positions of predicted SF1-binding site (Close boxes) on mouse *Fgf9* promoter firefly luciferase reporter constructs (Left). Reporter gene activity was shown as relative luciferase activity (fold activation) from each construct containing various putative SF1-binding site normalized to full length plasmid cotransfected with pCMV6-Entry (Right). All data are presented as means \pm SEM ($n = 4$), * $P < 0.05$; *** $P < 0.001$. (D) Relative luciferase activity measured from mouse *Fgf9* promoter construct (–1873/34) cotransfected with plasmids overexpressing Sry, Sf1, and Sox9. Data are shown as relative luciferase activity (fold activation) normalized to cotransfected with pCMV6-Entry. All data are presented as means \pm SEM ($n = 3$), * $P < 0.05$, ** $P < 0.01$, *** $P < 0.001$.

(Figure 2B, lanes 6 and 7), thus demonstrating that the complex was formed by SRY and the indicated sequence element. In parallel, EMSA was performed using oligonucleotides containing putative hSRE-8 (–175/–168 bp) sequences of the *FGF9* promoter region (Supplementary Figure S1B). Although a similar specific protein–DNA interaction was detected (Supplementary Figure S1B, lanes 1–5), SRY antibody failed to compete with the bindings of protein with the DNA element as indicated by the super-shifting band intensity compared with the nonspecific IgG control (Supplementary Figure S1B, lanes 6 and 7). These results therefore support that the predicted SRY-binding site hSRE-6, but not hSRE-8, is a functional SRY-binding element. Finally, we applied a site-directed mutagenesis assay to alter the SRY-binding site sequences within –833/–821 bp on the *FGF9* promoter region (R6mut construct, Figure 2C, upper panel). While the Luc RNA levels from both WT and R6mut cells are higher in SRY-overexpressing condition than the pcDNA-entry control, a substantial decrease from ~ 7 to ~ 3 -fold (a 56% decrease) of Luc RNA in R6mut cells was found in comparison to the WT cotransfected with SRY ($P < 0.01$, Figure 2C, bottom left). Consequently, a significant reduction of 20% luciferase activity was found in R6mut-transfected cells with SRY in comparison to the WT-transfected cells ($P < 0.05$, Figure 2C, bottom right). Taken together, these data demonstrate that SRY specifically binds to human *FGF9* promoter at position –833/–821 and upregulates *FGF9* mRNA expression through transcriptional activation.

As a previous study demonstrated that mouse SRY synergizes with SF1 to bind to *Sox9* testis-specific enhancer of *Sox9* core

(TESCO) region and upregulates *Sox9* expression during male testis development [37], the possibility of human SF1 being involved in SRY-mediated *FGF9* mRNA expression was also assessed. We first predicted the SF1-binding sites in the human *FGF9* promoter region and found three putative SF1-binding sites (Supplementary Table S1, Figure 2D, upper panel). By using reporter gene assays, we found that luciferase activities were similar between *FGF9* full-length promoter construct in COS7 cells either with or without overexpressing recombinant human SF1 ($P = 0.3049$, Figure 2D). The results suggest that human SF1 may not be involved in SRY-mediated *FGF9* mRNA expression. We then applied a ChIP assay to confirm the result of a lack of interaction between endogenous SF1 and human *FGF9* promoter *in vivo*. Fragmented chromatin was prepared from NT2/D1 cells and pulled down by using anti-SF1 antibody. This was followed by PCR with specific primer pairs to detect the amount of chromatin pulled down from various putative SF1-binding sites (Figure 2E, upper panel). Results of PCR from SF1-pulled down DNA fragments indicated that no differences were detected between SF1 and IgG-ChIP groups (Figure 2E and Supplementary Figure S1). On the other hand, a ~ 4 -fold enrichment of PCR products that target *AMH* promoter region (Figure 2F, upper panel), a known SF1 direct downstream gene, was obtained in SF1- compared with IgG-pulled down chromatins (Figure 2F bottom panel). These results indicate that human SF1 does not bind to *FGF9* promoter to control its expression. Collectively, our data provide evidence to show that human SRY binds to the hSRE sequences located on the *FGF9* promoter and activates *FGF9* mRNA expression.

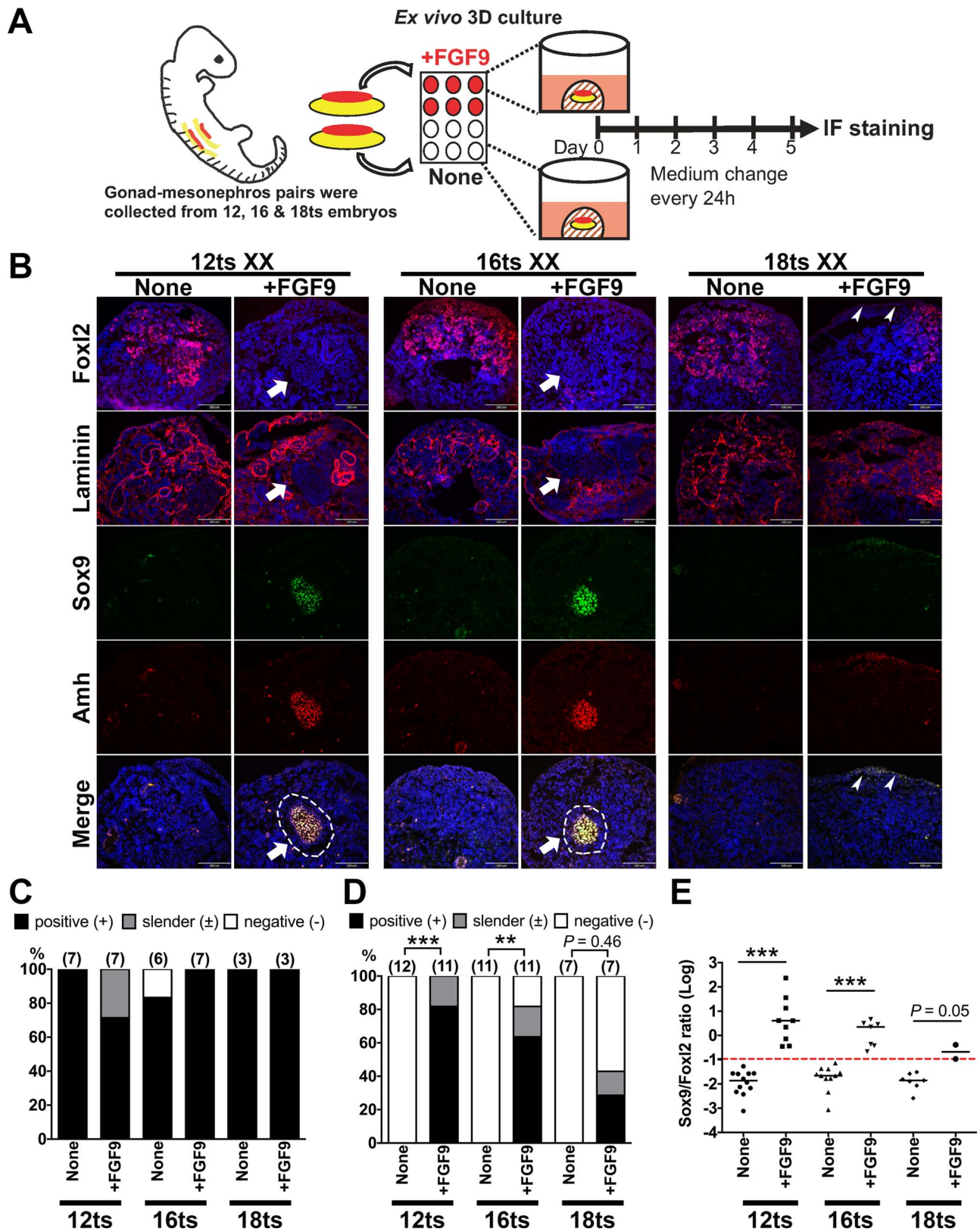


Figure 4. FGF9 repressed ovarian genes and promoted testicular characteristics in cultured 12–18 ts gonads. (A) *Ex vivo* 3D gonad culture flowchart. Paired mouse gonad–mesonephros were isolated from 12, 16, and 18 ts embryos and cultured in 12-well plates containing medium with or without recombinant FGF9 (50 ng/mL) for 5 days. Cultured gonads were fixed and serial cryosectioned for further analysis. (B) The cultured XX gonads from various stages (12, 16, and 18ts) were analyzed by IF for the presence of female supporting cell marker (Foxl2, red), and male supporting cell markers (Sox9, green, and AMH, red). Anti-laminin (red) was used to delineate the basement membrane of testis cords. Merge indicates combined Sox9 (green) and Amh (red) IF single (scale bar, 100 μ m).

Mouse SRY and SF1 cooperatively increase *Fgf9* promoter activity

We then tested whether SRY-mediated *Fgf9* expression can be observed in mice. We examined a ~2-kb interval within the mouse *Fgf9* promoter region (–1873/370 bp, NCBI accession number: NM_013518.4) for the presence of SRY-binding sites. Three putative SRY-binding sites were identified using two different bioinformatics prediction tools (Figure 3A and Supplementary Table S1). To examine whether these putative *Fgf9* mSREs interact with mouse SRY, serial deletion constructs containing different mSREs were fused to a luciferase reporter gene system, and luciferase activity under mouse SRY overexpression (Supplementary Figure S2A) was assayed in COS7 cells (Figure 3B). Compared with the –1873/370 construct, overexpression of SRY had no effect on reporter gene activity for constructs containing mSRE-1 and mSRE-2 (i.e., comparison between constructs –1873/370 and –1606/370, and between constructs –1873/370 and –1208/370). A further deletion from –1208 to –903 that deletes the putative mSRE-3 displayed a drastic decrease of luciferase activity in responding to SRY overexpression ($P < 0.01$). Taken together, these results suggest that the SRY regulation of *Fgf9* mRNA expression may occur through the direct binding onto the putative SRY-responsive element located within the –1010/–998 region (i.e., mSRE-3). Interestingly, similarly to the observation we found in humans, when we deleted the conserved uORF located on the 5'UTR of mouse *Fgf9*, luciferase activity was elevated to ~6-fold and even increased to up to ~16-fold under SRY overexpression. These data confirmed the strong inhibitory effect of uORF on the translation of *FGF9/Fgf9* mRNA.

The possibility of mouse SRY synergizing with SF1 to control *Fgf9* expression was explored. There were two putative SF1-binding sites (Figure 3C and Supplementary Table S1) were predicted from ~2-kb interval on mouse *Fgf9* promoter region. Using the reporter gene system, we found that the functional SF1-binding site is located on the –1150 to –1141 region, as a significant reduction of luciferase activity was observed when the –1208 to –903 region (putative SF1-binding site No. 1, $P < 0.001$) was deleted (Figure 3C). These results suggest that the mouse SF1 binds to the –1150/–1141 region of *Fgf9* promoter to control *Fgf9* mRNA expression. Next, we assayed luciferase activities in COS7 cells transfected with the full-length *Fgf9* promoter construct (–1873/34) under SRY and/or SF1 overexpression condition (Supplementary Figure S2A). As shown in Figure 3D, expression of SRY and SF1 alone activated promoter activity up to 2-fold ($P < 0.001$) and 4-fold ($P < 0.001$), respectively. A further increase of luciferase activity up to 5-fold was observed when both SRY and SF1 were coexpressed ($P < 0.001$, Figure 3D), indicating a synergistic regulation of these two TFs.

Interestingly, we found a roughly 2-fold (Figure 3D, $P < 0.001$) increases in promoter activity when the COS7 cells were cotransfected with mouse *Sox9* construct (Supplementary Figure S2A), whereas the predicted score of putative SOX9-binding sites within this region were all low and beyond the cutoff value of 85 (Supplementary Table S1). As SRY and SOX9 share 76% similarity in amino

acid sequences and are functionally compatible [38], we reasoning the observation may be likely due to the functionally interchangeable nature of DNA-binding domains between SRY and SOX9. To find out the possibility of existing long-range enhancer region like TESCO reported for mouse *Sox9* gene [39], we searched for SOX9 ChIP-Seq peaks in *FGF9/Fgf9* upstream regions in both human and mouse genomes. Using ChIP-Atlas [33], many TFs function in gonad or embryonic development were identified. For example, a cluster of ChIP-Seq peaks for Dmrt1 [40] were found in upstream 10–20 kb region from mouse *Fgf9* genomic region (Supplementary Figure S2B). However, we found no sign of SOX9 ChIP-Seq peak for up to ~100-kb regions from *Fgf9* TSS (Supplementary Figure S2B). Taken together, these results demonstrate that all three well-known gonadal TFs are capable to bind to mouse *Fgf9* promoter in vitro. Furthermore, mouse SRY cooperatively works with SF1 to bind *Fgf9* at –1150/–998 region to upregulate *Fgf9* mRNA expression.

Exogenous FGF9 culture has no effect on testis cord formation in XY gonads regardless of the development stage

Previously, the SRY direct downstream gene, SOX9, was found to be sufficient for functional testis development [41]. In addition, a gain of *FGF9* copy number was found in 46, XX SRY-negative male disorders of sex development (DSD) patients [24]. It would be interesting to know whether FGF9 signaling alone is sufficient to change cell fate and trigger male testis development. For this purpose, we first established an *ex vivo* 3D culture system (Figure 4A). Paired mouse gonad/mesonephros tissues with XX or XY chromosomes were isolated from 12, 16, and 18 ts embryos and cultured in 12-well plate containing medium with or without recombinant FGF9 (50 ng/mL). After a 5-day culture, IF staining was performed using tissue serial cryosections with antibodies against SOX9, AMH, and FOXL2, which are markers representing male Sertoli and female granulosa cells, respectively. In addition, laminin staining was used to delineate the basement membrane of testis cords. As expected, we did not detect FOXL2-positive cells in cultured XY gonads, regardless of the presence or absence of recombinant FGF9 from all developmental stages (Supplementary Figure S3A, top panel). In contrast, both SOX9 and AMH, a direct downstream target gene of SOX9, positive cells were clearly stained in good agreement with laminin-delineated spaces in XY gonads processed from serial sections (Supplementary Figure S3A, indicated panels) in both groups. Moreover, XY gonads cultured with additional FGF9 for 5 days showed similar morphology when compared with untreated control groups (12 and 16 ts) or minor oversize distortion of testis cord (18 ts). These results indicate that the extra dosage of FGF9 has no or very little effect on the appearance of testis characteristics observed in the XY gonads.

Exogenous FGF9 promotes male sexual fate in XX gonads within a critical time window

Next, we examined the effects of adding recombinant FGF9 in the cultured XX gonads. Interestingly, while FOXL2-positive cells

Figure 4. (continued) Dotted circle indicates well-defined testicular cord-like structure. Arrow indicates the relative position of testicular cord-like structure in the serial cryosections. Arrowhead indicates scattered cells expressing male-supporting cell markers. (C and D) Phenotype classifications and summary statistics from FGF9-cultured (C) XY and (D) XX gonads. The classified three groups are negative (–), positive (+), and slender (\pm) according to the previously used definition [25]. Stacking bar was plotted from the percentage of the presence of each class in the indicated group where the total number of animals was counted up to 100%. (E) Scatter dot was plotted with the ratio of expression of *Sox9* to *Foxl2* from different developmental stages. Only cultured XX gonads that show positive and negative phenotypes were included. The bar in each group indicates the medium from each indicated group. The red-dotted line represents the cutoff value of the ratio of expression of *Sox9* to *Foxl2* that enables the sex cell fate change from female to male.

were clearly detected in the granulosa cells of the XX gonads area (Figure 4B, top panel), a discontinuous and unorganized pattern of laminin distribution was found together with no SOX9/AMH expression in FGF9 (–) culture medium (i.e., none FGF9 group) from all developmental stages (Figure 4B, middle and bottom panels). In contrast, XX gonads cultured with recombinant FGF9 for 5 days significantly abolished FOXL2 protein expression in the developing granulosa cells, and a marked expression of SOX9/AMH was detected enclosed inside laminin-delineated spaces (Figure 4B, indicated panels). Nevertheless, it was noticed that XX gonads cultured in FGF9 (+) medium from 18 ts stage showed less SOX9/AMH-positive cells compared with the ones from 12 and 16 ts stages, and there was no well-defined testis cord formation as delineated by laminin staining (Figure 4B). We then classified cultured gonads into three different phenotypes according to the definition published previously [25]. While the positive and negative phenotypes were determined by whether cells were clearly stained with SOX9/AMH and with laminin-delineated space in the gonadal area, the slender phenotype represents an intermediate phenotype in which only a few SOX9/AMH positive cells were found in laminin-delineated spaces. The frequencies of the presence of different phenotypes in cultured XY and XX gonads were calculated. Although a few cases showed negative or slender phenotypes due to a failure of IF staining, almost all cultured XY gonads displayed positive phenotype regardless of the status of FGF9 addition and/or developmental stages (Figure 4C). On the other hand, all culture XX gonads in the no FGF9 medium group (i.e., none) showed complete absence of negative phenotype, whereas female gonads cultured in FGF9 (+) medium showed distinct patterns among different developmental stages (Figure 4D). The ability of FGF9-induced transformation (i.e., positive phenotype) is highest in the 12 ts stage (82%, $P < 0.001$), followed by 16 ts stage (64%, $P < 0.001$) and 18 ts stage (29%, $P = 0.46$). In order to further investigate cellular event that enables sex fate change, we measured the intensity of SOX9- and FOXL2-positive cells in cultured XX gonads from different stages. Compared with the untreated controls, we found that the intensity of SOX9-positive cells and FOXL2-positive cells were significantly increased to 12.9 and 5.3-fold ($P < 0.001$, Supplemental Figure S3B, left panel) and decreased to 5.2- and 4.6-fold ($P < 0.001$, Supplemental Figure S3B, right panel) in 12 and 16 ts gonads cultured with recombinant FGF9, respectively. Meanwhile, small differences in the intensity of FOXL2-positive cells ($P < 0.01$), and insignificant differences in SOX9-positive cells ($P = 0.09$), were found in 18 ts XX gonads in response to FGF9 addition (Supplemental Figure S3B). The ratio of SOX9 to FOXL2 from positive and negative phenotypes in each sample group was plotted using the intensity data. We found that XX gonads cultured under no recombinant FGF9 showed similar ratios among three development stage groups. On the other hand, significant increases of SOX9 to FOXL2 ratios that represent cell fate change in FGF9-treated XX gonads were observed in the 12–16 ts groups ($P < 0.001$, Figure 4E), whereas the difference between the two treatment groups at the 18 ts stage was marginal due to the small sample size ($P = 0.05$). A critical SOX9 to FOXL2 ratio of –1 was obtained to suggest a physiological cutoff value that allows switching on male cell lineage development. Taken together, these results indicate that FGF9 is sufficient to alter cell fate from female to male and to induce male testis cord formation. Nevertheless, the data also imply a critical time window within the 12–16 ts range, and a minimal expression level for the SOX9 to FOXL2 ratio to enable the transformation to take place.

Discussions

FGF9 is expressed in embryonic gonads of both sexes prior to embryonic day (E)11.5, at which time it is dismissed in wild type XX female gonads but upregulated in XY male gonads during sexual differentiation [20, 42]. Although previous studies demonstrated that FGF9 plays a crucial role in male sex development [43] and yet the control of FGF9 expression during the early embryonic stage in male gonads leading to concordant male sex development remains controversy. The hallmark study done by the Capel group has shown significant decrease or absence of *Fgf9* mRNA expression in SOX9 homozygous null mutant gonad using RNA in situ hybridization, whereas SRY expression was similar to the wild type [20]. The data provided genetic evidences to support that FGF9 expression is dependent on SOX9 in the early embryonic male gonad. Using antibody against mouse SRY and cells from E11.5 male gonad, at which time SRY was at its highest expression, Li et al. [29] applied whole-genome promoter tiling microarray (ChIP-Chip) and identified *Fgf9* as a downstream specific target gene of SRY. Hence the results demonstrated SRY binds to *Fgf9* and may control its expression. Interestingly, the same approach failed to precipitate *Fgf9* with SOX9 antibody from E12.5 male gonad, at which time SRY expression was at its minimum if it has not disappeared [29]. Nevertheless, the study also showed that several SRY-specific targets including *Fgf9* can respond to SOX9 stimulation in the promoter assay system, under transient overexpression of Sox9, presumably due to the functionally interchangeable nature of DNA-binding domains between SRY and SOX9 [29]. The authors proposed that SRY binds to specific set of target genes (i.e., *Fgf9*) to promote testis cord formation in early Sertoli cells. In turn, SRY passes on its functions to SOX9 to regulate common targets and activates its own gene regulatory program in sex determination. In fact, a recent study showed that mouse SOX9 directly binds to conserved genomic region of *Fgf9* promoter in E13.5 male gonad [44]. Collectively, results from these studies support the notion that both SRY and SOX9 are capable of binding onto *Fgf9* promoter and it may depend on the availability of these factors to determine the time and binding interaction between *Fgf9* and them.

During the early embryonic development, the differentiation of the bipotential gonad into a testis or ovary relies on several gene networks that are associated with male and female pathways. In the XY gonad, testicular development depends on SOX9 activation to promote Sertoli cell proliferation and differentiation [41], as well as FGF9 expression to repressing WNT4 signaling [43, 45]. The two events must occur analogously, sooner after SRY expression starting at E10.5, to ensure proper testis development. Kim et al. [20] proposed that SRY activates SOX9, and SOX9 upregulates FGF9. Such linear relationship among three genes seems to imply a sequential action in which male activation pathway advances from female repression pathways for 6–12 h due to the time required for transcriptional upregulate of SOX9 on *Fgf9* expression in XY gonads. In light of study reported by Li et al. [29] that found SRY binds to mouse *Fgf9* in E11.5 male mouse gonad, we thus like to propose an alternative regulation that SRY activates SOX9 and FGF9 simultaneously in the early developing male gonad; thus, both SOX9-activated and FGF9-repressed gene networks can be established in parallel and cooperatively to promote testis cord formation. As SRY only expresses in a short period of time and fade away quickly after E11.5, SOX9 takes control of gene regulatory program, including the positive feedback loop with FGF9, in sex determination. It's of notice that *in vitro* and/or *ex vivo* experiments may not always

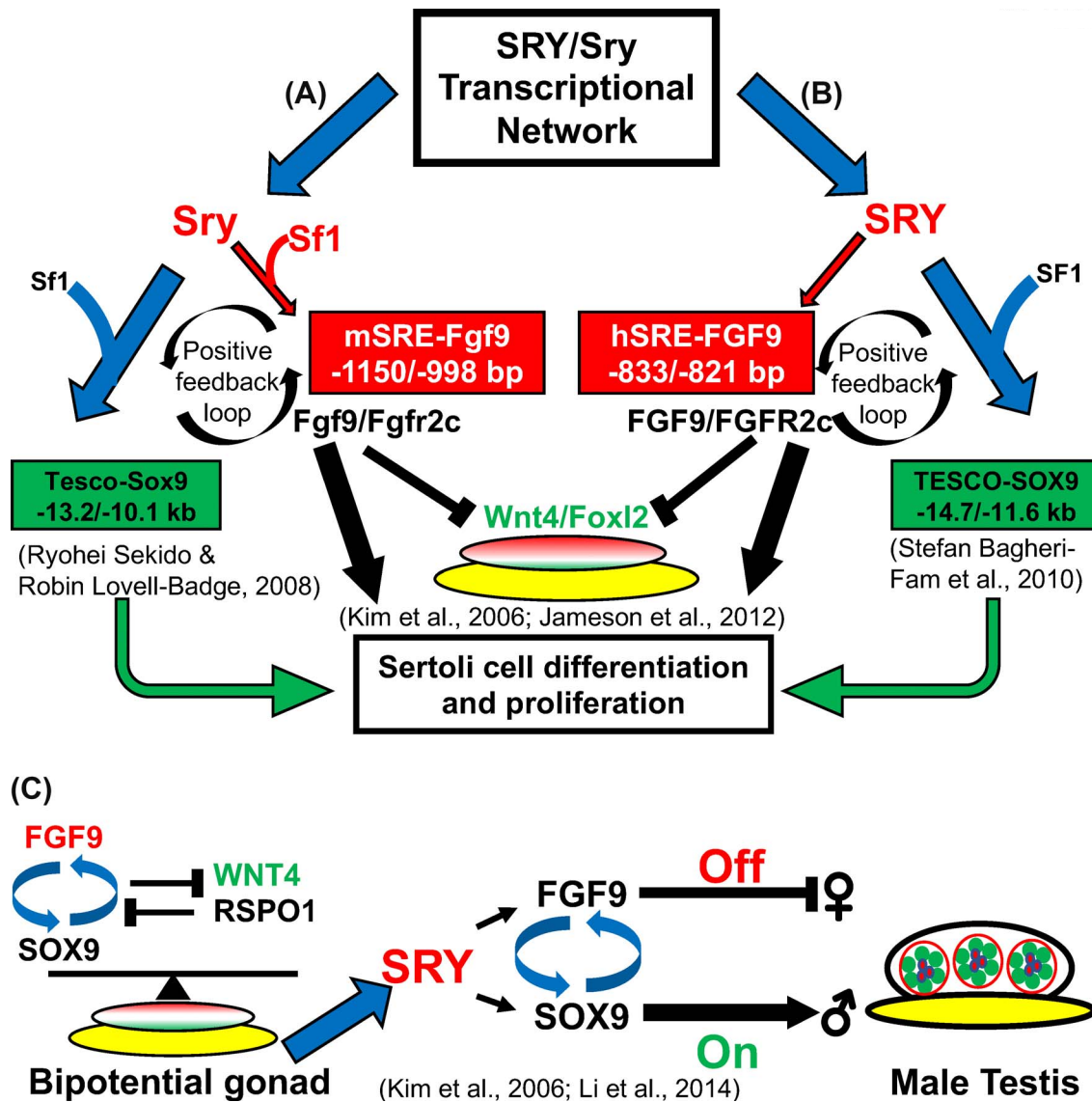


Figure 5. SRY transcriptional network governs male testis determination and development. SRY transcriptional network in (A) mouse and (B) human. (C) Male testis development requires SRY turn on high level of FGF9–FGFR2 signal to suppress female WNT4 and FOXL2 expression (black line, Off) and maintaining high FGF9–SOX9 expression to promote Sertoli cell differentiation and proliferation (black arrow, On).

reflect genetic roles in animals. Nevertheless, results from these studies demonstrate the dynamic and complicated regulatory networks controlled by SRY/SOX9 to exert appropriate actions to determine male sex fate in early sex-determining time window. The current study aimed to follow-up on the findings reported by Li et al. [29] to identify the regions of SRY binding onto *Fgf9* promoter. We predicted distinct sets of putative binding sites for SRY on *FGF9/Fgf9* 5' flanking regions and identified the SRY-responsive element located on –1010/–998 of mouse *Fgf9* and –833/–821 of human *FGF9* promoter regions. These results support that SRY directly binds to *FGF9/Fgf9* promoter and may have thus control its upregulation in early embryonic gonads. On the other hand, although the predicted scores of all putative binding sites for SOX9 on *FGF9/Fgf9* 5' flanking regions were much lower than that of SRY and SF1 (i.e., 70; except for one putative binding site on *FGF9/Fgf9* with a prediction score of 82.5), overexpression of mouse SOX9 enables to activate

luciferase activity to a similar magnitude like SRY. We speculate the results are owing to similar reason proposed by Li et al. [29]. Our data, together with previous findings, suggest that SRY upregulates FGF9 expression to exert its dual functions in activating the testicular differentiation and repressing the ovarian-determining program(s), respectively. Previous studies have shown that human SRY lacks the glutamine-rich domain that is reportedly important for mouse male sex determination [46, 47], suggesting that the model of SRY regulation on gene expression may differ between mice and humans. In agreement with this theory, our data showed that the putative SF1-binding sites are located within the –1150/–1141 region of mouse *Fgf9* promoter and cooperatively work with mouse SRY to control *Fgf9* mRNA expression, whereas the human SF1 neither binds to *FGF9* promoter nor regulates *FGF9* expression. As SRY has been shown to upregulate human monoamine oxidase A (MAOA) gene promoter activity either alone [48] or synergistically working

with WD repeat domain 5 (WDR5) to control SOX9 expression in male sex determination [49], these data together demonstrate that the transcriptional activity of SRY is content dependent, and human SRY may act with a more flexible regulation mechanism to control expression of downstream target genes.

FGF9 as an autocrine/paracrine growth factor is known to be involved in the physiological function of many cell types including Sertoli cells [17], Leydig cells [50], and germ cells [42] during testis development. Although previous studies demonstrated that *Fgf9* knockout mice showed a male-to-female sex reversal phenotype [19] and autosomal duplication of the human *FGF9* gene is associated with 46, XX SRY-negative DSD patient [24], whether FGF9 plays a sufficient role in male sex determination remains to be elucidated. Using an *ex vivo* 3D culture model, we provide evidence to demonstrate that FGF9, in the absence of SRY, is sufficient to fully activate not only the testis-determining pathway but also the downstream differentiation pathway, leading to the formation of a testis-like structure and turn sex fate from female to male in early embryonic development. Our data support the 46, XX SRY-negative DSD model observed in humans [24] and demonstrate the necessary and sufficient roles of FGF9 in male sex determination.

Our data showed that exogenous FGF9 triggers male testis cord formation in SRY-negative XX gonads within a critical time window of ~6 h, corresponding to 12–16 ts. In fact, the cultured 18 ts XX gonads displayed only a few SOX9/AMH-positive cells and no testis cord formation. These results are consistent with previous reports that FGF9 failed to induce SOX9 and AMH expression in E11.5 (~18 ts) XX gonads and consequently results in no or small male testis cord formation [27]. A recent study also showed that FGF9 is unable to trigger SOX9 expression, while it can still repress FOXL2 expression successfully in 11.5 days post coitum (d.p.c.) (18 ts) XX gonads. As a consequence, it failed to induce testis formation [27, 28]. The roughly 6-h critical time window has been proposed previously to show that even SRY, the master regulator in male testis development, initiates the switch of cell fate from female to male within the 12–16 ts stage (~6-h time window) in the *Hsp-Sry* transgenic mice [51]. In this study, we provide a new insight into the SRY transcriptional network of male sex determination. Nevertheless, the successful transformation from female cell lineage to male cell fate only occurs within a critical 6-h window, specifically approximately within the 12–16 ts (11–11.25 d.p.c.) interval in XX gonads. Outside this time window, FGF9 is insufficient to initiate male testis development in XX gonads. Together, these findings suggest that the 6-h time window is delimited by the ability to engage the high-FGF9/low-WNT4 signaling states. In other words, SRY-mediated FGF9 expression in early embryonic stage (i.e., 12–18 ts) is vital to suppress female WNT4 signaling [20, 43] and establish Sertoli cell differentiation and proliferation [19, 28] for the testis cord development.

In summary, we have identified hSRE and mSRE in *FGF9/Fgf9* promoter region and demonstrated that in the absence of SRY, FGF9 activates the male sex determination pathway and leads to the formation of testis cord in the cultured XX gonads. Combined information from the literatures and the results obtained from this study, the transcriptional networks in controlling male sex determination in early embryonic stage is provided (Figure 5A and B). Briefly, we identify mouse and human SRY, respectively, bind to -1010/-998 of mouse *Fgf9* promoter (Figure 5A, red arrow) and -833/-821 of human *FGF9* promoter (Figure 5B, red arrow) regions to promote *FGF9* expression and may thus suppress WNT4/FOXL2 signaling [20, 43, 45] and maintain SOX9 expression in a positive-feed

loop manner ([20]. Together with SRY-mediated SOX9 expression (Figure 5A and B, blue arrow) in human [37] and mouse [39, 52], the transcription network breaks the balanced expression in the bipotential gonad (Figure 5C). Through the upregulation of SOX9 for Sertoli cell differentiation and activation of FGF9 for ovarian pathway suppression, a switch to endorse male testis development occurs (Figure 5 upper panel, green arrow and black line, and C). The FGF9-SOX9-positive feedback loop maintains high expression of each other while SRY expression fades away to sustain male gonad development (Figure 5C) [20].

Supplementary data

Supplementary data are available at *BIOLRE* online.

Authors' contributions

YHL: Conducting the experiments and draft manuscript.
TMC: Construct plasmids and conducting the experiments.
BMH, SHY, CCW, YML, JIC: Supervising and analyzing data from animal and *ex vivo* studies.
SJT: Supervising and analyzing data from *in vitro* studies.
HSS: Designing and supervising the study, archiving and being responsible for all data, figures, and text related to basic characterization and profiling of FGF9.

Acknowledgements

The authors would like to thank the Bioinformatics Core at the National Cheng Kung University for providing assistances in computational analyses.

Conflict of interest

The authors have declared that no conflict of interest exists.

References

1. Kronenberg H, Williams RH. *Williams Textbook of Endocrinology*. Saunders: Elsevier; 2007.
2. Bastian C, Muller JB, Lortat-Jacob S, Nihoul-Fekete C, Bignon-Topalovic J, McElreavey K, Bashamboo A, Brauner R. Genetic mutations and somatic anomalies in association with 46,XY gonadal dysgenesis. *Fertil Steril* 2015; 103:1297–1304.
3. Sinclair AH, Berta P, Palmer MS, Hawkins JR, Griffiths BL, Smith MJ, Foster JW, Frischauf AM, Lovell-Badge R, Goodfellow PN. A gene from the human sex-determining region encodes a protein with homology to a conserved DNA-binding motif. *Nature* 1990; 346:240–244.
4. Lim HN, Freestone SH, Romero D, Kwok C, Hughes IA, Hawkins JR. Candidate genes in complete and partial XY sex reversal: Mutation analysis of SRY, SRY-related genes and FTZ-F1. *Mol Cell Endocrinol* 1998; 140:51–58.
5. Just W, Rau W, Vogel W, Akhverdian M, Fredga K, Graves JA, Lyapunova E. Absence of Sry in species of the vole *Ellobius*. *Nat Genet* 1995; 11:117–118.
6. Soullier S, Hanni C, Catzeflis F, Berta P, Laudet V. Male sex determination in the spiny rat *Tokudaia osimensis* (Rodentia: Muridae) is not Sry dependent. *Mamm Genome* 1998; 9:590–592.
7. Foster JW, Dominguez-Steglich MA, Guioli S, Kwok C, Weller PA, Stevanovic M, Weissenbach J, Mansour S, Young ID, Goodfellow PN. Campomelic dysplasia and autosomal sex reversal caused by mutations in an SRY-related gene. *Nature* 1994; 372:525–530.

8. Hammes A, Guo JK, Lutsch G, Leheste JR, Landrock D, Ziegler U, Gubler MC, Schedl A. Two splice variants of the Wilms' tumor 1 gene have distinct functions during sex determination and nephron formation. *Cell* 2001; 106:319–329.
9. Luo X, Ikeda Y, Parker KL. A cell-specific nuclear receptor is essential for adrenal and gonadal development and sexual differentiation. *Cell* 1994; 77:481–490.
10. Meeks JJ, Crawford SE, Russell TA, Morohashi K, Weiss J, Jameson JL. Dax1 regulates testis cord organization during gonadal differentiation. *Development* 2003; 130:1029–1036.
11. Rhen T, Metzger K, Schroeder A, Woodward R. Expression of putative sex-determining genes during the thermosensitive period of gonad development in the snapping turtle, *Chelydra serpentina*. *Sex Dev* 2007; 1:255–270.
12. Bashamboo A, McElreavey K. Human sex-determination and disorders of sex-development (DSD). *Semin Cell Dev Biol* 2015; 45:77–83.
13. Karkanaki A, Praras N, Katsikis I, Kita M, Panidis D. Is the Y chromosome all that is required for sex determination? *Hippokratia* 2007; 11:120–123.
14. DiNapoli L, Capel B. SRY and the standoff in sex determination. *Mol Endocrinol* 2008; 22:1–9.
15. Weksler NB, Lunstrum GP, Reid ES, Horton WA. Differential effects of fibroblast growth factor (FGF) 9 and FGF2 on proliferation, differentiation and terminal differentiation of chondrocytic cells in vitro. *Biochem J* 1999; 342:677–682.
16. Goldfarb M. Functions of fibroblast growth factors in vertebrate development. *Cytokine Growth Factor Rev* 1996; 7:311–325.
17. Willerton L, Smith RA, Russell D, Mackay S. Effects of FGF9 on embryonic Sertoli cell proliferation and testicular cord formation in the mouse. *Int J Dev Biol* 2004; 48:637–643.
18. Chen TM, Chen YH, Sun HS, Tsai SJ. Fibroblast growth factors: potential novel targets for regenerative therapy of osteoarthritis. *Chin J Physiol* 2019; 62:2–10.
19. Colvin JS, Green RP, Schmahl J, Capel B, Ornitz DM. Male-to-female sex reversal in mice lacking fibroblast growth factor 9. *Cell* 2001; 104:875–889.
20. Kim Y, Kobayashi A, Sekido R, DiNapoli L, Brennan J, Chaboissier MC, Poulat F, Behringer RR, Lovell-Badge R, Capel B. Fgf9 and Wnt4 act as antagonistic signals to regulate mammalian sex determination. *PLoS Biol* 2006; 4:e187.
21. Siggers P, Carre GA, Bogani D, Warr N, Wells S, Hilton H, Esapa C, Hajihosseini MK, Greenfield A. A novel mouse Fgfr2 mutant, hobbyhorse (hob), exhibits complete XY gonadal sex reversal. *PLoS One* 2014; 9:e100447.
22. Chen TM, Kuo PL, Hsu CH, Tsai SJ, Chen MJ, Lin CW, Sun HS. Microsatellite in the 3' untranslated region of human fibroblast growth factor 9 (FGF9) gene exhibits pleiotropic effect on modulating FGF9 protein expression. *Hum Mutat* 2007; 28:98.
23. Chung CL, Lu CW, Cheng YS, Lin CY, Sun HS, Lin YM. Association of aberrant expression of sex-determining gene fibroblast growth factor 9 with Sertoli cell-only syndrome. *Fertil Steril* 2013; 100:1547–1554.
24. Chiang HS, Wu YN, Wu CC, Hwang JL. Cytogenetic and molecular analyses of 46,XX male syndrome with clinical comparison to other groups with testicular azoospermia of genetic origin. *J Formos Med Assoc* 2013; 112:72–78.
25. Hiramatsu R, Harikae K, Tsunekawa N, Kurohmaru M, Matsuo I, Kanai Y. FGF signaling directs a center-to-pole expansion of tubulogenesis in mouse testis differentiation. *Development* 2010; 137:303–312.
26. Bradford ST, Wilhelm D, Bandiera R, Vidal V, Schedl A, Koopman P. A cell-autonomous role for WT1 in regulating Sry in vivo. *Hum Mol Genet* 2009; 18:3429–3438.
27. Gustin SE, Stringer JM, Hogg K, Sinclair AH, Western PS. FGF9, activin and TGFbeta promote testicular characteristics in an XX gonad organ culture model. *Reproduction* 2016; 152:529–543.
28. Schmahl J, Kim Y, Colvin JS, Ornitz DM, Capel B. Fgf9 induces proliferation and nuclear localization of FGFR2 in Sertoli precursors during male sex determination. *Development* 2004; 131:3630:3627–3636 Epub Jun 2004.
29. Li Y, Zheng M, Lau YF. The sex-determining factors SRY and SOX9 regulate similar target genes and promote testis cord formation during testicular differentiation. *Cell Rep* 2014; 8:723–733.
30. Hacker A, Capel B, Goodfellow P, Lovell-Badge R. Expression of Sry the mouse sex determining gene. *Development* 1995; 121:1603–1614.
31. Hiramatsu R, Kanai Y, Mizukami T, Ishii M, Matoba S, Kanai-Azuma M, Kurohmaru M, Kawakami H, Hayashi Y. Regionally distinct potencies of mouse XY genital ridge to initiate testis differentiation dependent on anteroposterior axis. *Dev Dyn* 2003; 228:247–253.
32. Oki S, Ohta T, Shioi G, Hatanaka H, Ogasawara O, Okuda Y, Kawaji H, Nakaki R, Sese J, Meno C. ChIP-atlas: a data-mining suite powered by full integration of public ChIP-seq data. *EMBO Rep* 2018; 19.
33. Chen TM, Shih YH, Tseng JT, Lai MC, Wu CH, Li YH, Tsai SJ, Sun HS. Overexpression of FGF9 in colon cancer cells is mediated by hypoxia-induced translational activation. *Nucleic Acids Res* 2014; 42:2932–2944.
34. Knower KC, Sim H, McClive PJ, Bowles J, Koopman P, Sinclair AH, Harley VR. Characterisation of urogenital ridge gene expression in the human embryonal carcinoma cell line NT2/D1. *Sex Dev* 2007; 1:114–126.
35. Gau BH, Chen TM, Shih YH, Sun HS. FUBP3 interacts with FGF9 3' microsatellite and positively regulates FGF9 translation. *Nucleic Acids Res* 2011; 39:3582–3593.
36. Yen WH, Ke WS, Hung JJ, Chen TM, Chen JS, Sun HS. Sp1-mediated ectopic expression of T-cell lymphoma invasion and metastasis 2 in hepatocellular carcinoma. *Cancer Med* 2016; 5:465–477.
37. Sekido R, Lovell-Badge R. Sex determination involves synergistic action of SRY and SF1 on a specific Sox9 enhancer. *Nature* 2008; 453:930–934.
38. Bergstrom DE, Young M, Albrecht KH, Eicher EM. Related function of mouse SOX3, SOX9, and SRY HMG domains assayed by male sex determination. *Genesis* 2000; 28:111–124.
39. Gonen N, Quinn A, O'Neill HC, Koopman P, Lovell-Badge R. Normal levels of Sox9 expression in the developing mouse testis depend on the TES/TESCO enhancer, but this does not act alone. *PLoS Genet* 2017; 13:e1006520.
40. Buonocore F, Clifford-Mobley O, King TFJ, Striglioni N, Man E, Suntharalingham JP, Del Valle I, Lin L, Lagos CF, Rumsby G, Conway GS, Achermann JC. Next-generation sequencing reveals novel genetic variants (SRY, DMRT1, NR5A1, DHH, DHX37) in adults with 46,XY DSD. *J Endocr Soc* 2019; 3:2341–2360.
41. Qin Y, Bishop CE. Sox9 is sufficient for functional testis development producing fertile male mice in the absence of Sry. *Hum Mol Genet* 2005; 14:1221–1229.
42. Bowles J, Feng CW, Spiller C, Davidson TL, Jackson A, Koopman P. FGF9 suppresses meiosis and promotes male germ cell fate in mice. *Dev Cell* 2010; 19:440–449.
43. Jameson SA, Lin YT, Capel B. Testis development requires the repression of Wnt4 by Fgf signaling. *Dev Biol* 2012; 370:24–32.
44. Rahmoun M, Lavery R, Laurent-Chaballier S, Bellora N, Philip GK, Rossitto M, Symon A, Pailhoux E, Cammas F, Chung J, Bagheri-Fam S, Murphy M et al. In mammalian foetal testes, SOX9 regulates expression of its target genes by binding to genomic regions with conserved signatures. *Nucleic Acids Res* 2017; 45:7191–7211.
45. Bagheri-Fam S, Bird AD, Zhao L, Ryan JM, Yong M, Wilhelm D, Koopman P, Eswarakumar VP, Harley VR. Testis determination requires a specific FGFR2 isoform to repress FOXL2. *Endocrinology* 2017; 158:3832–3843.
46. Bowles J, Cooper L, Berkman J, Koopman P. Sry requires a CAG repeat domain for male sex determination in *Mus musculus*. *Nat Genet* 1999; 22:405–408.
47. Zhao L, Quinn A, Ng ET, Veyrunes F, Koopman P. Reduced activity of SRY and its target enhancer Sox9-TESCO in a mouse species with X*Y sex reversal. *Sci Rep* 2017; 7:41378.
48. Wu JB, Chen K, Li Y, Lau YF, Shih JC. Regulation of monoamine oxidase a by the SRY gene on the Y chromosome. *FASEB J* 2009; 23:4029–4038.

49. Xu Z, Gao X, He Y, Ju J, Zhang M, Liu R, Wu Y, Ma C, Lin Z, Huang X, Zhao Q. Synergistic effect of SRY and its direct target, WDR5, on Sox9 expression. *PLoS One* 2012; 7:e34327.
50. Lin YM, Tsai CC, Chung CL, Chen PR, Sun HS, Tsai SJ, Huang BM. Fibroblast growth factor 9 stimulates steroidogenesis in postnatal Leydig cells. *Int J Androl* 2010; 33:545–553.
51. Hiramatsu R, Matoba S, Kanai-Azuma M, Tsunekawa N, Katoh-Fukui Y, Kurohmaru M, Morohashi K, Wilhelm D, Koopman P, Kanai Y. A critical time window of Sry action in gonadal sex determination in mice. *Development* 2009; 136: 129–138.
52. Bagheri-Fam S, Sinclair AH, Koopman P, Harley VR. Conserved regulatory modules in the Sox9 testis-specific enhancer predict roles for SOX, TCF/LEF, Forkhead, DMRT, and GATA proteins in vertebrate sex determination. *Int J Biochem Cell Biol* 2010; 42: 472–477.